Chapter 4

Beyond the primary wave field

Summary

Whereas chapter (3) presents a theory for the primary wave field, we turn now the attention to a wave field description that also includes the early part of the coda. Because the coda contains mainly the incoherent field, not the wave field itself is the quantity of interest but the ensemble averaged envelope. The advantage of self-averaging cannot be used in the following. Therefore, we do not consider this as a part of the extended O'Doherty-Anstey theory. Nevertheless, this characterization of seismogram envelopes is also based on the Rytov approximation. More precisely, we formulate the two frequency mutual coherence function based on the wave field approximation which we obtained in the previous chapter. To compare our results with existing theories and 2-D finite-difference simulations we derive also the two frequency mutual coherence function in the Markov approximation for 2-D random media. This coherence function can be used in order to describe seismogram envelopes as shown in Sato and Fehler (1998). A more general introduction to the theory of coherence functions can be found in Born and Wolf (1999).

In section (4.1) we review the formulation of the two frequency mutual coherence function in the Markov approximation and present its solution for plane waves in 2-D Gaussian correlated random media. The formulation of the two-frequency mutual coherence function using the Rytov- and Bourret-approximation is presented in section (4.2).

4.1 Evolution of seismogram envelopes

It is well-known that seismic pulses traveling through heterogeneous media experience a change of their envelopes. Sato and Fehler (1998) described the broadening of seismogram envelopes due to multiple scattering with help of the Markov approximation. The latter is, like the Rytov approximation, based on the parabolic wave equation and includes therefore multiple forward scattering effects. They obtained the intensity spectral density, whose Fourier transform corresponds to the temporal evolution of the mean square of a bandpass-filtered trace recorded at a certain depth inside the random medium. Similar formulations of the intensity pulse propagation can be found in Ishimaru (1978) and Sheng et al. (1990).

Let us consider the intensity of an initially plane wave field at a certain depth z in a 2-D random media (the transverse coordinate is x). Using the Fourier transform of the wave field with respect to time (denoted by $U(\omega, x, z)$), we can write the intensity in the following way:

$$I_t(t,z) = \frac{1}{(2\pi)^2} \int_{-\infty}^{\infty} d\omega' \int_{-\infty}^{\infty} d\omega'' \, \langle U(\omega', x, z) U^\star(\omega'', x, z) \rangle \, e^{-i(\omega'-\omega'')(t-z/c_0)} \, . \tag{4.1}$$

The two-frequency coherence function is defined by

$$\Gamma_2 = \langle U(\omega', x, z) U^\star(\omega'', x, z) \rangle \, , \tag{4.2}$$

i. e., the two-frequency mutual coherence function at the same spatial position. Therefore, equation (4.1) becomes

$$\begin{aligned} I_t(t,z) &= \frac{1}{(2\pi)^2} \int_{-\infty}^{\infty} d\omega_c \int_{-\infty}^{\infty} d\omega_d \, \Gamma_2(\omega', \omega'', x=0, z) \, e^{-i\omega_d(t-z/c_0)} & (4.3) \\ &= \frac{1}{2\pi} \int_{-\infty}^{\infty} d\omega_c \, \hat{I}(t, \omega_c) \quad , & (4.4) \end{aligned}$$

where ω_c and ω_d are center of mass and difference coordinates, respectively. So the intensity spectral density $\hat{I}$ is given by the Fourier transform of Γ_2:

$$\hat{I}(t, \omega_c, z) = \frac{1}{2\pi} \int_{-\infty}^{\infty} d\omega_d \, \Gamma_2(\omega', \omega'', x=0, z) \, e^{-i\omega_d(t-z/c_0)} \, . \tag{4.5}$$

The remaining task is to determine Γ_2. This was done by Sato and Fehler (1998) for the plane wave case in 3-D and by Fehler et al. (2000) for point-source radiation in 2-D. In the case of a plane wave in 2-D random media, we show in appendix D that

$$\Gamma_2 = {}_0\Gamma_2 \; e^{-k_d^2 A(0) z/2} \tag{4.6}$$

with

$${}_0\Gamma_2 = \sqrt{\operatorname{sech}\left[2\exp(i3\pi/4)\sqrt{k_d/k_m}\right]} \quad , \tag{4.7}$$

where $k_d = \omega_d/c_0$, $k_m = \frac{2k_c^2 a_\perp^2}{L}$ with $k_c = \omega_c/c_0$ and $a_\perp$ the transversal correlation length. The corresponding result in 3-D random media reads

$${}_0\Gamma_2 = \operatorname{sech}\left[2\exp(i3\pi/4)\sqrt{k_d/k_m}\right] \quad . \tag{4.8}$$

Note that $\hat{I}$ is not dependent on ω_c if we assume Gaussian correlated heterogeneities. In general this is not the case. In Fig. (4.1) the intensity spectral density is computed for

several travel distances inside a 2-D Gaussian random medium. As expected, the broadening of envelopes with increasing travel-distance can be observed.

Note that equation (4.5) describes the output intensity due to a δ-pulse as input intensity I_i and can be therefore understood as the corresponding Green's function. If $\hat{I}$ is not dependent on ω_c (which is the case for Gaussian correlated random media), the output intensity can be expressed as a convolution integral of the input intensity (Ishimaru, 1978, chapter 15):

$$\begin{aligned} I_t(t,z) &= \int_{-\infty}^{\infty} dt'\, \hat{I}(t-t',z) \cdot I_i(t', z=0) \\ &= \hat{I}(t,z) * I_i(t, z=0)\,. \end{aligned} \tag{4.9}$$

Ishimaru calls this case the wide-sense stationary uncorrelated scattering channel.

In seismology, one does not exactly know the input signal (source signal). To model the temporal evolution of seismogram envelopes, equation (4.5) can be interpreted in the following sense: The summation over all frequencies ω_c corresponds to the measured intensity, i.e, to the seismogram envelope. Applying a bandpass filter to the seismograms before constructing the envelope reflects a small portion of I_t that is approximately given by $\hat{I}$. Thus, $\hat{I}$ is the mean square of a band-pass filtered trace (the MS envelope), whose frequency content is represented by ω_c. With this recipe Scherbaum and Sato (1991) modeled the broadening of seismogram envelopes in order to estimate the statistical properties of lithospheric heterogeneities in Honshu, Japan.

In Fig. (4.2) we compare the analytical result (4.5) with seismogram envelopes from 2-D plane wave simulations in Gaussian correlated random media. Here, we know the input intensity and can use equation (4.9). Convolving the intensity spectral density function with the square of the input-wavelet results in the black curves in Fig. (4.2). The corresponding numerically determined envelopes are shown by the grey curves. The agreement between theory and experiment is good for small travel-distances and gets worse with increasing L. The reason for this behavior is that for large travel-distances the neglect of backscattered waves is not justified. Moreover, in the given experiment the dominant wavelength is only slightly smaller than the correlation length. Choosing $ka \gg 1$ yields much better agreement between experiment and theory. This has been demonstrated by Fehler et al. (2000) by means of similar numerical experiments.

From the above given derivation it becomes clear that I_t describes the temporal evolution of the intensity for the ensemble of all random medium realizations. It is not appropriate to describe single realizations of seismogram envelopes. The factorization of Γ_2 in (4.6) and the fact that $\exp(-k_d^2 A(0) z/2)$ accounts for the effect of ensemble averaging lead Sato and Fehler (1998) to the conclusion that ${}_0\Gamma_2$ reflects the properties of a single realization. This argument is however not convincing because Γ_2 is by definition an ensemble averaged quantity. Indeed, the term $\exp(-k_d^2 A(0) z/2)$ accounts for the effects of phase fluctuations (wandering effect in the terminology of Lee and Jokipii, 1975), but these effects cannot be treated separately when evaluating the integral (4.5).

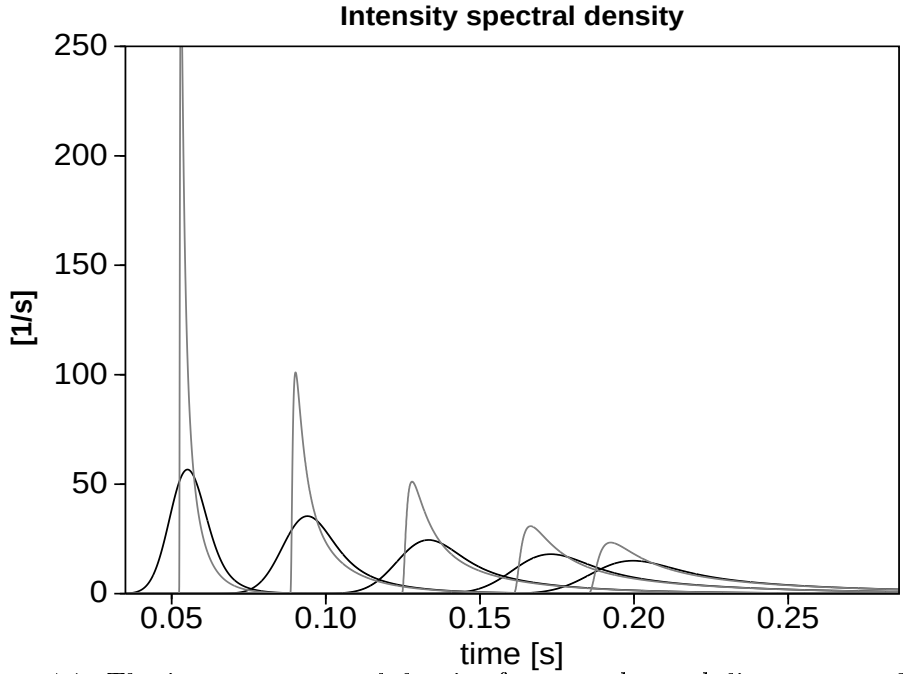

Figure 4.1: The intensity spectral density for several travel-distances inside a 2-D Gaussian random medium ($c_0 = 3000m/s, \sigma = 0.1, a = 40m$) according to equation (4.5). The black curves are obtained when Γ_2 is used as in equation (4.6). Skipping the exponential term in equation (4.6) and then computing $\hat{I}$ yields the grey curves.

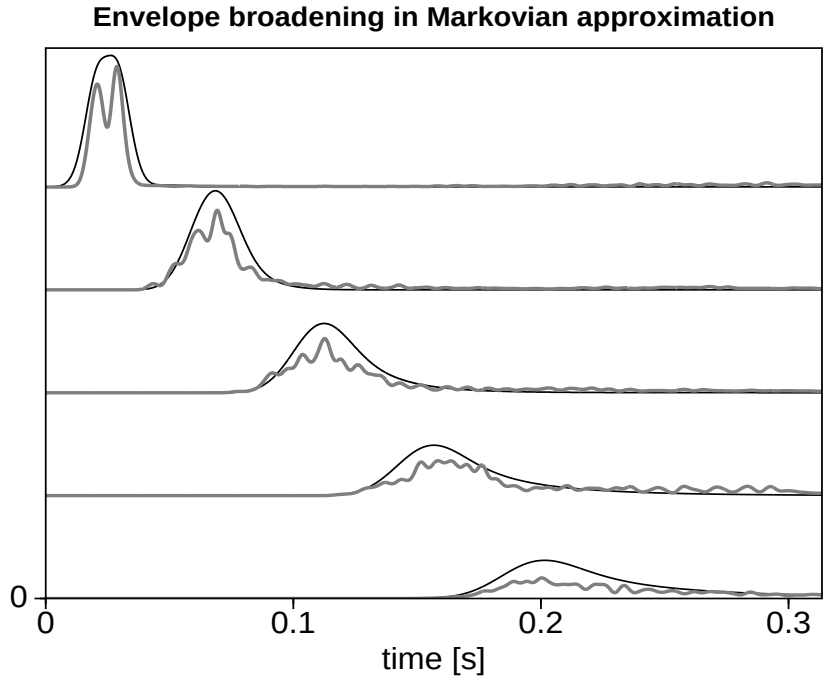

Figure 4.2: The envelope broadening in the Markovian approximation. The grey curves correspond to numerically determined averaged seismogram envelopes in a 2-D Gaussian random medium ($c_0 = 3000m/s, \sigma = 0.15, a = 45m$) for the travel-distances $L = 56, 176, 296, 416, 536m$. In the uppermost envelope the deterministic form of the input intensity is observable. That is why for small travel-distances the wave field is not yet 'randomized'. The black curves are computed using equation (4.9).

4.2 Envelope broadening in the Rytov approximation

In this section it is shown that the two-frequency coherence function can be formulated using the wave field attributes derived in chapter (3). This results in an alternative, new description of ensemble averaged seismogram envelopes.

Let's start with the definition of the two-frequency coherence function:

$$\Gamma_2(\omega', \omega'') = \langle U(\omega', x, z) U^\star(\omega'', x, z) \rangle$$

and recall the Rytov transformation in equation (3.8)

$$U = U_0 e^{\Psi}$$

where the incident wave field is given by

$$U_0 = A_0 e^{i\phi_0}$$

with a constant amplitude $A_0 = 1$ and phase $\phi_0 = kz$ for propagation in z-direction. Inserting equation (4.10) into the definition of Γ_2 yields

$$\Gamma_2(\omega', \omega'') = \langle U_{0_1}\, e^{\Psi_1}\; U^\star_{0_2}\, e^{\Psi^\star_2} \rangle \,. \tag{4.10}$$

To keep the equations short, we introduce the subscripts $1, 2$ on the righthand side of this and the following equations referring to the dependency on the frequencies ω', ω''. Since the incident wave field is a non-random quantity the latter equation becomes

$$\Gamma_2(\omega', \omega'') = e^{i(\phi_{0_1} - \phi_{0_2})} \langle e^{\Psi_1 + \Psi^\star_2} \rangle \,. \tag{4.11}$$

If $\Psi_1 + \Psi_2^\star$ is Gaussian distributed then we can write

$$\Gamma_2(\omega', \omega'') = e^{i(\phi_{0_1} - \phi_{0_2})}\, e^{\langle \Psi_1 \rangle + \langle \Psi^\star_2 \rangle}\, e^{\frac{1}{2}\left\langle \left[\Psi_1 + \Psi^\star_2 - \langle \Psi_1 + \Psi^\star_2 \rangle \right]^2 \right\rangle} \,. \tag{4.12}$$

To see this, note that for a Gaussian random variable x with its probability density function $p(x)$ the following identity holds

$$\begin{aligned} \langle e^x \rangle &= \int_{-\infty}^{\infty} dx\, e^x p(x) \\ &= \int_{-\infty}^{\infty} dx\, e^x \frac{1}{\sqrt{2\pi}\sigma_{xx}} e^{-\frac{(x - \langle x \rangle)^2}{2\sigma^2_{xx}}} \\ &= e^{\langle x \rangle + \frac{\sigma^2_{xx}}{2}} \\ &= e^{\langle x \rangle}\, e^{\frac{1}{2}\left\langle (x - \langle x \rangle)^2 \right\rangle} \,. \end{aligned} \tag{4.13}$$

Since $\Psi = \chi + i\phi$, the assumption of a Gaussian distribution is justified (see also the discussion in section 2.3). Moreover, the PDF of the sum of Ψ_1 and $\Psi_2^\star$ is given by the convolution their PDF's which results in a Gaussian distribution provided that Ψ_1 and $\Psi_2^\star$ are Gaussian distributed. If we substitute the approximations for the logarithmic wave field attributes presented in equations (3.17) and (3.18), i.e

$$\begin{aligned} \langle \chi \rangle &= -\sigma^2_{\chi\chi} \quad , \\ \langle \phi \rangle &= \phi_c - \phi_0 - \sigma^2_{\chi\phi} \quad , \end{aligned}$$

and recall the definition of the (cross-) variance

$$\begin{aligned}
\langle \Psi_1^2 \rangle - \langle \Psi_1 \rangle^2 &= \sigma^2_{\chi_1\chi_1} - \sigma^2_{\phi_1\phi_1} + 2i\sigma^2_{\chi_1\phi_1} \\
\langle \Psi_2^{\star 2} \rangle - \langle \Psi_2^{\star} \rangle^2 &= \sigma^2_{\chi_2\chi_2} - \sigma^2_{\phi_2\phi_2} - 2i\sigma^2_{\chi_2\phi_2} \\
\frac{1}{2}\left(\langle \Psi_1 \Psi_2^{\star} \rangle - \langle \Psi_1 \rangle \langle \Psi_2^{\star} \rangle\right) &= \sigma^2_{\chi_1\chi_2} + \sigma^2_{\phi_1\phi_2} + i[\sigma^2_{\chi_2\phi_1} - \sigma^2_{\chi_1\phi_2}] \,,
\end{aligned}$$

one obtains from equation (4.12)

$$\Gamma_2(\omega', \omega'') = e^{\bar{\Psi}} = e^{\bar{\chi} + i\bar{\phi}} \tag{4.14}$$

with

$$\bar{\chi} = -\frac{1}{2}\left[\sigma^2_{\chi_1\chi_1} + \sigma^2_{\chi_2\chi_2} + \sigma^2_{\phi_1\phi_1} + \sigma^2_{\phi_2\phi_2}\right] + \sigma^2_{\chi_1\chi_2} + \sigma^2_{\phi_1\phi_2} \tag{4.15}$$

$$\bar{\phi} = \phi_{c_1} - \phi_{c_2} + \sigma^2_{\chi_2\phi_1} - \sigma^2_{\chi_1\phi_2} \,. \tag{4.16}$$

Equation (4.14) is lengthy but of a simple structure. All quantities are of the order $\mathcal{O}(\epsilon^2)$. The quantities $\sigma^2_{\chi\chi}, \sigma^2_{\phi\phi}, \sigma^2_{\chi\phi}$ and the coherent phase ϕ_c we know already from chapter 3 and are listed in appendix B.1. New terms are the two-frequency variances $\sigma^2_{\chi_1\chi_2}, \sigma^2_{\phi_1\phi_2}, \sigma^2_{\chi_1\phi_2}$. They can be calculated from the two-frequency correlation functions which have been obtained by Ishimaru (1978, chapter 19) and are discussed in appendix D.2. The resulting expressions for $\bar{\chi}$ and $\bar{\phi}$ show the same structure than the logarithmic wave field attributes presented in appendix B (see equations (B1)-(B3)). Moreover, for Gaussian correlated random media explicit results can be obtained. The intensity spectral density obtained in this approximation is shown in Figure (4.3) for the case of a Gaussian correlated random medium.

To verify the approximation (4.14) we use the same numerical experiment as in the previous section. The results are displayed in Figure (4.4), where a slight improvement regarding the agreement between theory and experiment can be observed (compare with Figure (4.2)).

There are several advantages in computing the seismogram envelopes based on the approximation (4.14). First of all, arbitrary fluctuation spectra may be inserted in equation (4.14). The formulation presented in this section uses plane waves. Note that the wave field approximations (3.17) and (3.18) are also valid for spherical waves. Thus, using the corresponding expressions for spherical waves, one can also apply formula (4.14). Finally, note that in the same way the two-frequency coherence function based on the causal wave field attributes (3.29) and (3.30) can be obtained which accounts for backscattering and is therefore superior to the presented approaches. This is, however, a topic for future research.

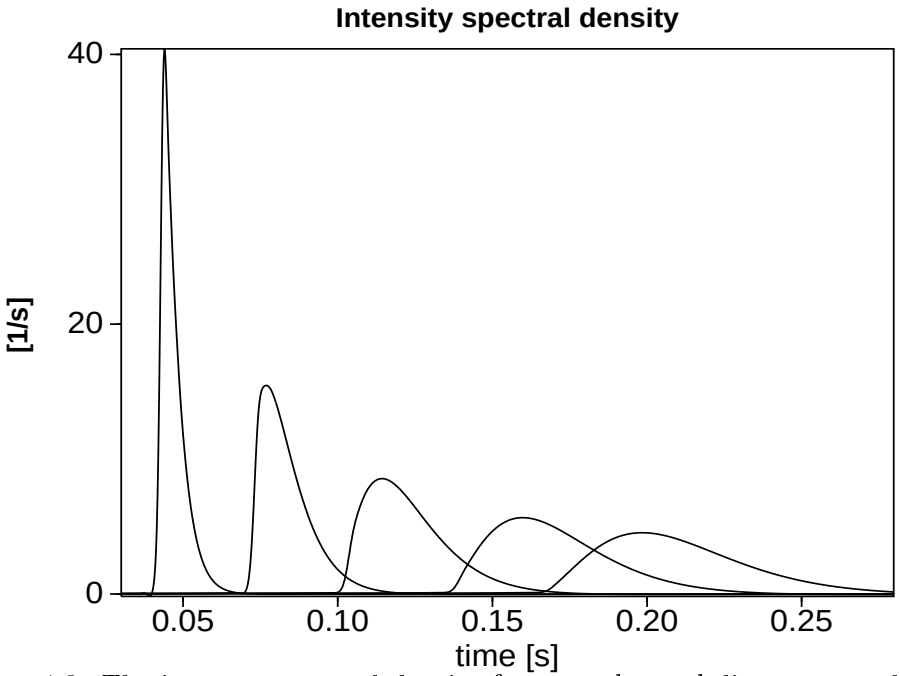

Figure 4.3: The intensity spectral density for several travel-distances inside a 3-D Gaussian random medium ($c_0 = 3000m/s, \sigma = 0.15, a = 40m$) according to equation (4.5) however using the two-frequency coherence function (4.14).

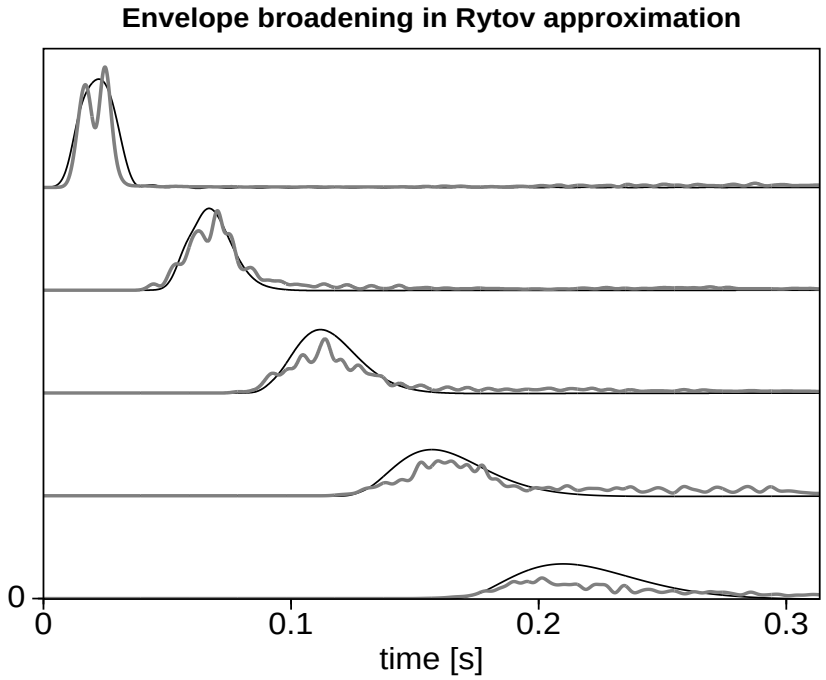

Figure 4.4: The envelope broadening in the Rytov approximation using the approximation (4.14) is denoted by the black curves. The grey curves correspond the same numerical experiment as in Figure (4.2). The dominant frequency of the input-wavelet is $70Hz$ and accordingly we choose $k_c = 0.12$. Compared with Figure (4.2), the agreement between theory and experiment is slightly improved.